Nanocoral PbS thin film growth by solid-vapor deposition

A. S. OBAID[a,b,*], M. A. MAHDI[a,c], Z. HASSAN[a]

[a]*Nano-Optoelectronics Research and Technology Laboratory*
School of Physics, Universiti Sains Malaysia, 11800 USM, Penang, Malaysia
[b]*Department of physics college of Sciences University of Anbar P.O.box PO. (55 431), Baghdad, Iraq*
[c]*Physics Department, College of Science, Basrah University, Basrah, Iraq*

Nanocoral PbS thin films were synthesized by vapor-solid deposition. Lead sulfide powder was first prepared and then heated in a tube furnace at 1323.15 K (1050 °C), and the resultant vapor was carried to the quartz substrate zone by an argon flow. The structural properties of the powder and the films were investigated using X-ray diffraction. The grain sizes of 11 and 41nm for both the powder and the nanocoral were obtained, respectively. The surface morphology of the powder and thin films were studied by electron scanning microscopy (SEM) and the micrographs revealed that the films are very adherent on the substrate with nanocoral-like shaped. The direct optical band gap of the nancoral PbS and powder were determined from optical transmittance measurements to be 0.37 and 0.4 eV, respectively.

1. Introduction

Nanometer-sized semiconductor particles have attracted considerable attention over the past few years because of their unique physical properties. Their optical and electrical properties are different from those of the bulk, resulting in new applications [1]. Lead sulfide (PbS) is an important binary IV–VI semiconductor material with a narrow direct optical energy gap (0.41 eV at 300 K) and relatively large Bohr excitation radius (18 nm), which provides a strong quantum confinement for both electrons and holes [2]. PbS is an important material for a variety of applications, such as infrared (IR) detectors, electroluminescent devices, solar cells, and other optoelectronic devices [3-6]. Hence, interest in developing techniques for the preparation of PbS thin films has been increasing. The physical method used in the current study to grow a crystal is solid-vapor or material vapor deposition. One of the major advantages of this method is that each of the operating parameters can be selected from a wide range, leading to a great variety of film structures [7]. Two types of mechanisms, namely, vapor-liquid-solid (VLS) and vapor-solid (VS) are available. In principal, the VLS mechanism is characterized by the presence of metal particles which cap at the nanostructure tip. The most important advantage for VLS growth mechanism is the possibility of obtaining various shapes in addition to the controlled growth in one dimension. On the other hand, its disadvantages are its high-temperature requirement, and that the material used as the catalyst affects the device. However, no metal catalyst is used in the current PbS nanocrystalline synthesis, and the vapor-solid mechanism is assumed instead of the VLS model [8]. In the current study, the noncatalytic fabrication of PbS nanocrystallites

by thermal evaporation (solid-vapor deposition technique), in which the required temperatures are attainable in a short time, is reported. Furthermore, the structural and optical properties of the PbS nanocorals were investgated.

2. Experiment details

PbS nanopowder were prepared by chemical bath deposition (CBD) technique. Initially the powder was prepared, lead acetate dissolved in 20 ml methanol and also thiourea was dissolved in 20 ml methanol, then we add thiourea solution to the lead acetate solution with drop wise. The mixed solution was stirred, heated at 80 C for about 30 min. After that the dark chocolate color powder of PbS is formed. The powder was treated several times with methanol and then dried in vacuum. To prepare thin films, 1 gm of PbS nanopowder was weighting by electrical balance. Nanocorals PbS was deposited on substrate quartz using the solid-vapor deposition process, in which PbS powder and argon gas flow were employed. The substrate quartz at first was clean washed with acetone, finally the substrate was cleaned ultrasonically with water. Argon gas flow was used to purify the tube, and then the sample was placed inside the tube while the gas was continuously injected into the system at the rate of 500 sccm (0.5 cm^3/min) for argon. After that PbS powder was placed in a small ceramic boat as the source, and placed in quartz tube 4cm diameter and 110 cm length inside the control hot zone of tube furnace. The substrate was placed in another boat about 5cm from the source along the direction of Ar flow. The source and substrate were heated at 1050 [0]C for 30-90 min under constant flow

of Ar gas 500sccm. The process ran for three hours. Room temperature is preferable for cooling.

3. Results and discussion

3.1 Structural characteristics

X-ray diffraction patterns of the prepared powder and thin films are shown in Fig. 1. All synthesized thin films exhibit cubic rock salt (NaCl) type structure. The diffraction peaks observed at 2θ of 25°, 30°, 43°, 50°, 53°, and 60° correspond to the (111), (200), (220), (311), and (222) planes of the cubic zinc blend phase of PbS, respectively, as confirmed by the (ASTM) card (No. 030660020). The main features of the diffraction patterns are the same, with only the peak intensity varying; the (111) and (200) peaks are the highest. The texture coefficient (*TC*) represents the texture of the particular plane, deviation of which from unity implies the preferred growth [9]. Quantitative information on the preferential crystallite orientation was obtained from another texture coefficient *TC*(*hkl*), which is defined as [10]

$$TC(hkl) = \frac{\frac{I(hkl)}{I_o(hkl)}}{\sum_n \frac{I(hkl)}{I_o(hkl)}} \times 100\% \qquad (1)$$

where *I*(*hkl*) is the measured relative intensity of plane *hkl*, I_o(*hkl*) is the standard intensity of plane *hkl* based on the ASTM file card No. 030660020, and *n* is the number of diffraction peaks. *TC*(*hkl*)=1 represents films with randomly oriented crystallites, whereas higher values indicate the abundance of grains oriented in a given *hkl* direction. The variation in TC of the peaks of the cubic lattice is presented in Table 1. The highest TC values for the powder and thin films were in the (200) plane. Table 1

shows that the PbS powder and the prepared PbS nanocorals have intensities different from those recorded in the ASTM for the PbS powder; however, no change in their positions was observed. This result can be explained by the presence of some kind of preferential orientation of the crystallites; that is, the formation of texture in the prepared films. The sharp XRD peaks indicate that the thin films have good crystalline structure. The diffraction peaks of the nanocorals becomes sharper compared with those of the powder, and without the creation of new phases in addition to that of PbS. These results suggest that no oxidation has occurred. Therefore, the quality of the crystallites has been improved [11].
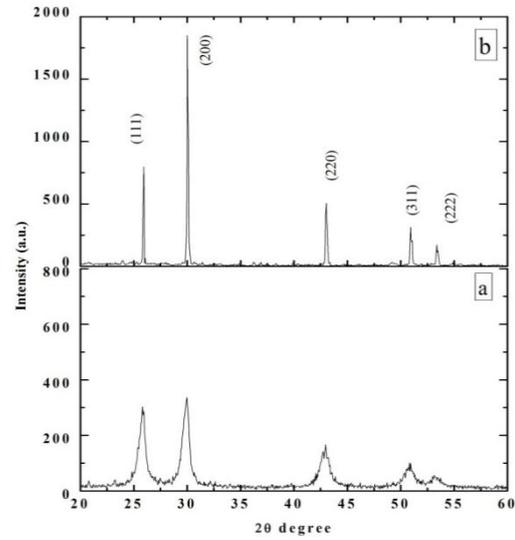
Fig. 1. XRD pattern of PbS :(a) powder, (b) nanocoral.

Table 1. The structural properties and energy gap of PbS nanocoral thin films.

sample	hkl	TC%	I/I$_O$	d(A) calculated	d(A) ASTAM	a(A) calculated	Eg(eV)	Gs(nm) Scherrer	Gs(nm) Brus Model
powder	111	6.93	78.00	2.981	2.970	5.930	0.42	11	10
	200	7.11	100.0						
nanocoral	111	4.56	66.05	2.970	2.969	5.936	0.37	41	35
	200	5.81	100.0						

The lattice constant of the PbS powder and the nanocoral thin films were calculated using the following relationship for the cubic phase structure [9]:

$$a = d(h^2 + k^2 + l^2)^{\frac{1}{2}} \qquad (2)$$

where *h*, *k*, and *l* are the Miller indices and *d* is the interplanar spacing. Table 1 shows that the lattice constant increased compared with the bulk film, clearly indicating the crystal formation under the effect of stress, which leads to the compression of the lattice constant [4, 5].

The grain sizes of the PbS powder and the nanocoral thin films were determined using Scherrer's formula [4], as follows:

$$Gs = \frac{k\lambda}{\beta\cos\theta} \qquad (3)$$

where k is a constant (0.94), λ is the wavelength of the XRD, and β is the full width at half maximum of the diffraction peak corresponding to a particular plane crystal; the value was obtained using the diffraction pattern in a direction perpendicular to the (200) plane. The grain size of the PbS powder is less than that of the nanocoral thin film, this finding is more promising compared with other. Rafea et al. [12] prepared nanostructured PbS powder with crystallite sizes of 52 nm.

3.2 Morphology

The surface morphology of the PbS nanocoral thin films on quartz can be observed in the SEM images shown in Fig. 2a. The results show that all the thin films exhibit uniform surface morphology over the entire substrate and that the films are of good quality. The crystals display a nanocoral structure. The small particles of the crystal clearly confirm the nanocrystalline nature. Yuanhua Ding et al. [13] reported on the synthesis of hollow and branch-like PbS microstructures. Zhiliang Xiu et al. [14] synthesized PbS nanocrystals with rod-like structures a sonochemical method. Patil et al.[15] reported on the synthesis of PbS nanopaticles using layer by-layer ion desorption and reaction.

The elemental analysis for the films was conducted using EDX, the atomic percentage of Pb is 49.65 and S is 50.35, as shown in Fig. 2b. The thin film is of good quality and does not contain common impurities, which is consistent with the results shown in the XRD patterns.
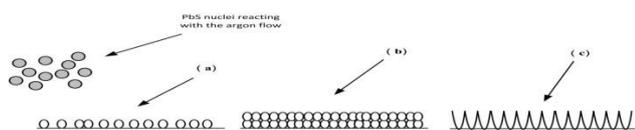
Fig. 2. (a) Adsorbed PbS nuclei on the substrate; (b) supersaturation; and (c) splitting (growth in various directions) of the nanocoral structure.

To explain the mechanism of growth of the deposited PbS nanocoral structure, the vapor-solid mechanism is proposed instead of the conventionally used vapor-liquid-solid (VLS) model. The PbS particles continuously evaporate from the quartz boat during the heating process. In the absence of oxygen and in the presence of argon, the PbS vapors are adsorbed on the surface of the quartz tube, react with the argon flow, and are then transported to the substrate to form PbS nuclei. As the reactant concentration increases, the PbS nuclei continue to combine and stack on one another as the reaction progresses, resulting in supersaturation and eventually in the splitting and growth

of the crystals in various directions. The resulting crystals take the form of nanocorals, indicating the dominance of this mechanism.

Element	Weight%	Atomic%
S K	13.56	50.35
Pb M	86.44	49.65
Totals	100.00	
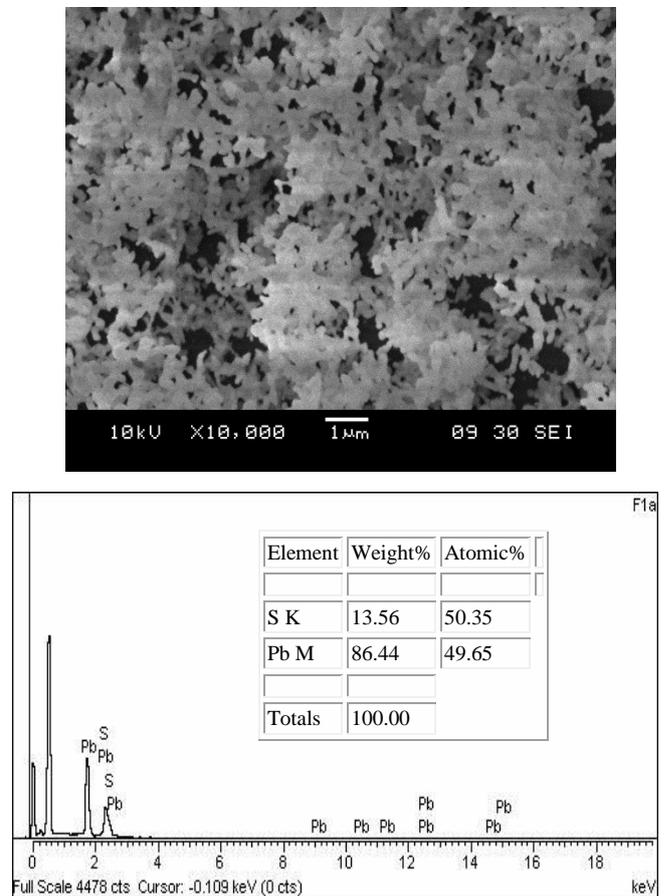
Fig. 3. SEM and EDX analysis of nanocoral PbS thin films.

3.3 Optical properties

The optical properties of the PbS nanocoral thin films and powder were studied using FTIR and measured after obtaining the IR absorbance and transmittance spectra. The absorbance data were used to evaluate the absorption coefficient (α) using the following equation [16]:

$$\alpha = 2.303 \times \frac{A}{t} \qquad (2)$$

where t is the thickness of the sample. The optical α (cm^{-1}) was calculated in the 2000 nm to 5000 nm wavelength range for both the nanocorals and the powder. Fig. 4 shows that the α values were higher than 10^5 cm^{-1}, indicating that PbS has a direct band gap and that the absorption coefficient for the nanocorals is higher than that for the powder but decrease below a certain wavelength for all samples. This value is reasonable for a semiconductor [15].
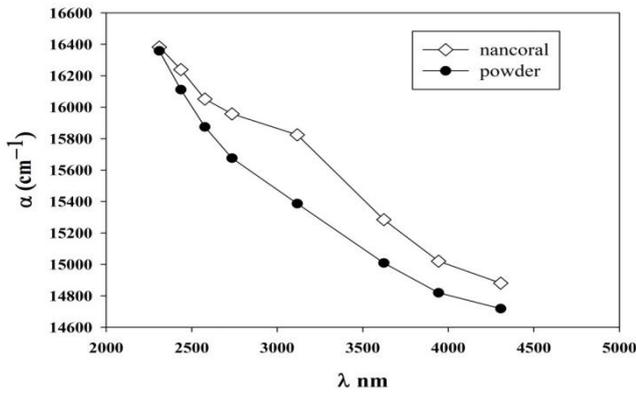
Fig. 4. Absorption coefficient as a function of wave length λ nm.

The energy gaps of the PbS nanocoral thin films were determined using the Tauc formula [16], as follows:

$$(\propto h\nu) = A^*(h\nu - E_g)^m \quad (3)$$

where A^* is constant, $h\nu$ is the incident photon energy, and the parameter m depends on the transmission type and is equal to $\frac{1}{2}$ for the allowed direct transmission. Fig. 5 shows a plot of $(\propto \times h\nu)^2$ vs hν. For the PbS thin films, the maximum of the valence band and the minima of the conduction band lie at the same k value in the $E–k$ band diagram, indicating that the transitions are the direct type. The energy gap was determined by extrapolating the linear portion. The Eg for the nanocoral PbS is determined to be 3351 nm (0.37 eV), which is less than that for the powder at 3100 nm (0.4 eV). As the grain size changes below a certain limiting size associated with its exciton Bohr radius, the spacing between the band levels also changes, thereby changing the value of E_g [12]. The grain size can be calculated from the retaliation between particle radius and band gap of nanostructure as given by Brus Model [12]

$$E_g(films) = E_g(bulk) + \frac{h^2\pi^2}{2R^2}\left(\frac{1}{m_e^*} + \frac{1}{m_h^*}\right) - \frac{1.786e^2}{\xi R} \quad (4)$$

In this equation, R is the radius of particle radius, m_e^*, m_h^* are the effective masses of the electron in the conduction band and of the hole in the valence band respectively, and $\xi = 17.3$ is the dielectric constant of PbS. The second term is the quantum localization (i.e. the kinetic energy) term, shifts E_g to higher energies. The third term arises from the screened Coulomb interaction between the electron and the hole, which shifts E_g to lower energies. The last term which is size independent, is associated with spatial correlation effects and is usually small in both its value and its effect on E_g. Moreover, it is usually small in both its value and its effect on E$_g$, where an increase in grain size results in a decrease in band gap Eg. It was observed that the grain size determined by Brus model have the same behavior to the values which were

determined using XRD, where the grain size of the PbS powder is less than that of the nanocoral thin film.
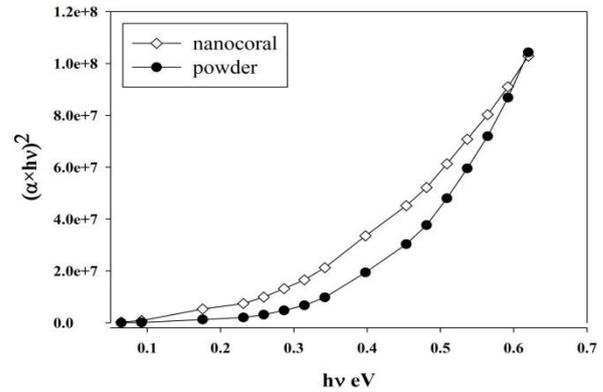
Fig. 5. ($\propto \times h\nu$)^2 as a function of photon energy hν.

4. Conclusion

The noncatalytic and template-free vapor deposition process have been used to prepare PbS. XRD analysis shows that all thin films are polycrystalline, pure and crystallize within a cubic rock salt (NaCl) type structure. The grain size of the PbS powder is smaller than that of the nanocoral structure thin film. SEM observations reveal that the films are very adherent on the substrate with nanocoral-like shaped. EDX results confirm the good quality of the thin films, without any commonly encountered impurities. These results are consistent with those of the XRD analysis. The Eg for the nanocoral PbS is determined to be 0.37 eV, which is less than that for the powder 0.4 eV.

References

[1] A. S. Obaid, M. A. Mahdi, Asmiet Ramizy, Z. Hassan, Advanced Materials Research **364**, 60 (2012).
[2] O. Madelung, Semiconductor:Data Handbook. springer, 2004. 3rd ed.
[3] X. Lui, M. Zhang. International journal of Infrared and Millimeter waves, **21**,1697(2000).
[4] E. Pentia, L. Pintilie, I. Matei, T. Botila, E. Ozbay, Optoelectronics & Advanced Materials 3, 525 (2001).
[5] P. K.. Basu, T. K. Chauduri, K. C. Nandi, R. S. Saraswat, H. N. Acharya, Journal of Materials Scienc **25**, 4014 (1990).
[6] S. Kumar, H. Khan Zishan, M. A. Majeed Khan, M. Husain. Current Applied Physics **5**, 561 (2005).
[7] C. Suryanayana, Non-equilibrium processing of materials, Pergamon Materials Series Langford Lane

Kidlington Oxford, UK, 1999. 2: p. 257.

[8] F. Wang, L. Virginia Wayman, A. Richard Loomis, E. Buhro William. ACS Nano, **5**, 5188 (2011).

[9] M. Caglar, Y. Caglar, S. Ilican, J. Optoelectron. Adv. Mater. **8**, 1410 (2006).

[10] H. Z. Zhang, X. C. Sun, R. M. Wang, D. P. Yu. Journal of Crystal Growth **269**, 464 (2004).

[11] M. M. Abbas, A. Ab-M. Shehabb, A-K. Al-Samuraeec, N-A. Hassanb. Energy Procedia **6**, 241 (2011).

[12] M. A. Rafa, N. Rousdy. Philosophical Magazine Lettersl **90**(2), 113(2010).

[13] Y. Ding, X. Liu, R. Guo, J. Cryst. Growth **307**, 145 (2007).

[14] Z. Xiu, Suwen Liu, Jiaoxian Yu, Fengxiu Xu, Weina Yu, Guangjian Feng. J. Alloy. Compd **457**, L11 (2008).

[15] R. S. Patil, C. D. Lokhande, R. S. Mane, T. P. Gujar, Sung-Hwan Han. J of G.Non-cryst.Solid **353**, 1645 (2007).

[16] A. Kadhim, A. Hmood, H. Abu. Hassan, Materials letters **65**, 3105 (2011).

_____

*Corresponding author: ahmed_s_alqasy@yahoo.com